2017 International Symposium on Nonlinear Theory and Its Applications,
NOLTA2017, Cancun, Mexico, December 4-7, 2017

Reconstruction of Bifurcation Diagrams using Time-series Data Generated by Electronic Circuits of the Rössler Equations

Yoshitaka Itoh† and Masaharu Adachi‡

Department of Electrical and Electronic Engineering, Tokyo Denki University
5 Senju-Asahicho Adachi-ku, Tokyo 120-8551, Japan
Email: †16ude01@ms.dendai.ac.jp, ‡adachi@eee.dendai.ac.jp

Abstract—We describe how to reconstruct bifurcation diagrams from time-series data generated by electronic circuits. The reconstructed bifurcation diagrams are estimates of the oscillatory patterns of the time series when the system parameters are changed. Bifurcation-diagram reconstruction could be used for parametric engineering and physical systems in the real world. In this study, we show that bifurcation diagrams can be reconstructed from time-series data generated by an electronic circuit of the Rössler equations. In addition, we estimate the Lyapunov exponents of the reconstructed bifurcation diagrams.

1. Introduction

In 1994, Tokunaga *et al.* [1] proposed reconstructing a bifurcation diagram (BD) by estimating the number of significant parameters of the target system and recognizing oscillatory patterns when its parameters are changed. Since then, several research groups have studied the reconstruction of BDs from time-series data generated by numerical experiments [2]–[7]. However, BD reconstruction could also be applied to real-world systems such as engineering and physical systems.

In this paper, as a precursor to tackling such real-world systems, we reconstruct BDs by using several time-series datasets generated by electronic circuits that realize the Rössler equations [8]. This follows on from our previous work in which we reconstructed the BDs of the Rössler equations from numerical data [9]. In addition, we estimate the Lyapunov exponents of the reconstructed BDs. We have previously proposed a method for this that involves a Jacobian matrix of time-series predictors [9]. However, in the present study, we employ the estimation method proposed by Wolf *et al.* [10], which can estimate the largest Lyapunov exponent from time-series data alone, even if the target dynamical system is unknown.

The rest of this paper is organized as follows. In Section 2, we explain the method for reconstructing BDs [1]. In Section 3, we explain the concept of an extreme learning machine (ELM), and in Section 4 we explain our estimation method. In Section 5, we describe the electronic-circuit realization of the Rössler equations, and in Section 6 we present the results of our numerical experiments. Finally, we draw conclusions in Section 7.

2. Reconstruction of Bifurcation Diagrams

In this section, we summarize the method for reconstructing a BD proposed by Tokunaga *et al.* [1]. We begin by taking several time-series datasets and making time-series predictors for them based on ELMs, from which we obtain the trained synaptic weights of the output neurons. Here, the synaptic weights and biases of the hidden neurons for the time-series predictors are generated randomly and then held fixed throughout the reconstruction process. The time-series predictors are described by

$$\mathbf{o} = P\left(\boldsymbol{\beta}^{(n)}, \mathbf{x}\right),\ (1 \leq n \leq N), \tag{1}$$

where $P(\cdot,\cdot)$ is a nonlinear map of the time-series predictors and N is the number of time-series datasets.

Next, we obtain eigenvalues and eigenvectors by applying a principal component analysis (PCA) [11] to the trained synaptic weights of the output neurons. To estimate the number of significant parameters, we calculate the cth cumulative contribution ratio by

$$CCR_c = \frac{\sum_{i=1}^{c} \lambda_i}{\sum_{j=1}^{C} \lambda_j},\ (1 \leq c \leq C), \tag{2}$$

where λ_j is the jth eigenvalue and C is the number of learned synaptic weights. The number of significant parameters, A, is estimated to be c when the cth cumulative contribution ratio is above 80%. The new synaptic weights of the output neurons are obtained for the principal components by

$$\tilde{\boldsymbol{\beta}} = U\boldsymbol{\gamma} + \bar{\boldsymbol{\beta}}, \tag{3}$$

where $U \in \mathbb{R}^{C\times A}$ is the matrix of eigenvectors $[\mathbf{u}_1\mathbf{u}_2 \cdots \mathbf{u}_A]$, $\mathbf{u}_i \in \mathbb{R}^C$ is the ith eigenvector, $\boldsymbol{\gamma} \in \mathbb{R}^A$ is an estimated parameter, and $\bar{\boldsymbol{\beta}}$ is an average of the synaptic weights of the output neurons.

Finally, we reconstruct the BD with the new synaptic weights of the output neurons. The nonlinear map of new time-series predictors for the BD reconstruction is described by

$$\mathbf{o} = P\left(\tilde{\boldsymbol{\beta}}, \mathbf{x}\right). \tag{4}$$

To reconstruct the BD, we generate time-series data repeatedly using the new time-series predictors while changing the estimated parameters.

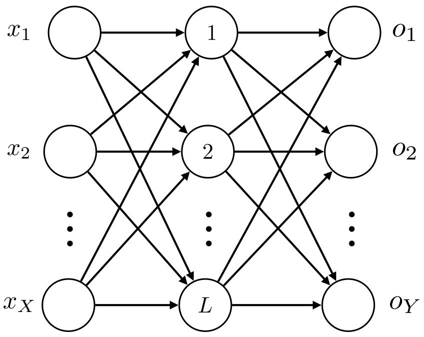

Figure 1: Structure of an ELM.

3. Extreme Learning Machine

In 2006, Huang *et al.* [12] proposed the concept of an ELM, which is a three-layer neural network whose structure is shown in Fig. 1. The learning algorithm of an ELM uses linear regression for the synaptic weights of the unbiased output neurons. The synaptic weights and the biases of the hidden neurons are generated randomly and are not trained. An ELM learns extremely quickly and has a good generalization performance in spite of its relatively simple structure.

The output of the lth hidden neuron $h_l \in \mathbb{R}$ is

$$h_l = g\left(\mathbf{w}_l^T \mathbf{x} + b_l\right), \tag{5}$$

where $\mathbf{w}_l \in \mathbb{R}^X$ and $b_l \in \mathbb{R}$ are the synaptic weights and the bias, respectively, of the lth hidden neuron, $\mathbf{x} \in \mathbb{R}^X$ is an input vector, and $g(\cdot)$ is a nonlinear function, for which we use the following sigmoid function in this study:

$$g(\chi) = \frac{\sigma}{1 + exp(-\zeta\chi)} - \epsilon, \tag{6}$$

where σ, ζ, and ϵ are parameters that are used to adjust the range of the sigmoid function to one of the target time series. The output $o_y \in \mathbb{R}$ of the yth output neuron is

$$o_y = \boldsymbol{\beta}_y^T \mathbf{h}, \tag{7}$$

where $\boldsymbol{\beta}_y \in \mathbb{R}^L$ are the synaptic weights for the yth output neuron and $\mathbf{h} = [h_1\ h_2\ \cdots\ h_L]^T$ is the output of the hidden neurons.

4. Estimation of Lyapunov Exponents from Time-series Data

In this study, we use the method proposed by Wolf *et al.* [10] to estimate Lyapunov exponents from time-series data. The estimation method directly measures the growth of the distance between points on two orbits. Figure 2 shows a schematic diagram of the estimation method, the algorithm for which is as follows. Here, this method uses the orbit of embedded time series data.

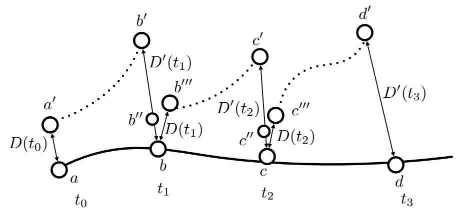

Figure 2: Schematic diagram of the method proposed by Wolf *et al.* [10] for estimating Lyapunov exponents.

1. Select an initial point a and a neighboring point a', and calculate the distance $D(t_0)$ between a and a'.
2. Calculate the distance $D'(t_1)$ between b and b', which are the corresponding points at time t_1 on the orbits emanating from points a and a'.
3. Calculate the vector bb'' as the normalized vector of $D'(t_1)$.
4. Find a neighboring point b''' of point b'', and calculate the distance $D(t_1)$ between b and b'''.
5. Repeat steps 2–4 until the predetermined time t_F.
6. Estimate the Lyapunov exponent by

$$\mu = \frac{1}{t_F - t_0} \sum_{k=1}^{F} log_2 \frac{D'(t_k)}{D(t_{k-1})}. \tag{8}$$

5. Electronic-circuit Realization of the Rössler Equations

The Rössler equations [8] are

$$\begin{aligned} \frac{d\xi}{d\tau} &= -\eta - \nu, && (9) \\ \frac{d\eta}{d\tau} &= \xi + \iota\eta, && (10) \\ \frac{d\nu}{d\tau} &= \kappa + \nu(\xi - \rho), && (11) \end{aligned}$$

where ι, κ, and ρ are parameters. In this study, we fix $\iota = 0.3$ and $\kappa = 0.31$, and use ρ as the bifurcation parameter. Figure 3 shows the electronic circuits used in this study. We modified the electronic circuits from Ref. [13] to be able to adjust the parameters using voltages V_ι, V_κ, and V_ρ shown in Fig. 3. Here, the voltages V_ι, V_κ, and V_ρ correspond to the parameters ι, κ, and ρ, respectively. Therefore, the BD is generated while changing the voltage V_ρ. The upper panel of Fig. 4 shows the BD generated by the electronic circuits. Here, the voltage ξ was measured with a sampling frequency of 25 kHz. In addition, the lower panel of Fig. 4 shows the estimated largest Lyapunov exponents. From Fig. 4, we see a correspondence between the Lyapunov exponents and the BD in that the Lyapunov exponents in cyclic regions are close to zero, whereas those in chaotic regions are definitely positive.

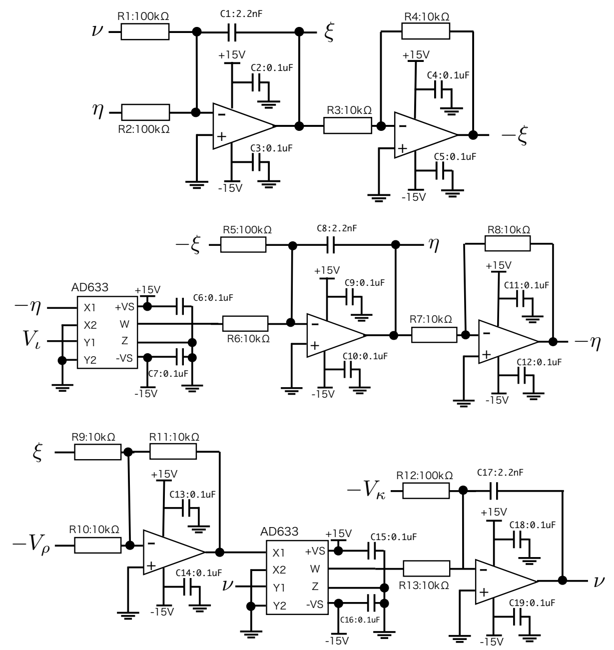

Figure 3: Electronic circuits to realize the Rössler equations.

6. Numerical Experiments

In this section, we present the results of reconstructing BDs from time-series data generated by the electronic-circuit realization of the Rössler equations. Firstly, we show a BD of the Rössler equations generated numerically using Matlab®. We then compare this with the BD generated by the electronic circuits, before presenting the reconstructed BD.

6.1. Bifurcation diagram of the Rössler equations considering a time factor

For comparison with the BD generated by the electronic circuits, we show the corresponding BD generated numerically in Matlab®. Considering the time factor of the electronic circuits, we modify the Rössler equations as follows:

$$\frac{d\xi}{d\tau} = \alpha(-\eta - \nu), \tag{12}$$

$$\frac{d\eta}{d\tau} = \alpha(\xi + \iota\eta), \tag{13}$$

$$\frac{d\nu}{d\tau} = \alpha(\kappa + \nu(\xi - \rho)), \tag{14}$$

where the time factor $\alpha = 220 \times 10^3$ is calculated from $\alpha = 1/CR$, where the capacitance $C = 2.2$ nF and the resistance $R = 100$ kΩ. The time-series datasets were generated using a third-order Runge–Kutta method in which the time increment was $\Delta\tau = 10^{-6}$. We then used the ξ-component time series sampled at steps of $40\Delta\tau$.

Figure 5 shows the BD generated in Matlab®, which we consider corresponds to the BD shown in Fig. 4. However, the BD shown in Fig. 4 might have been influenced by noise; for example, the range of the parameter values that exhibits the window might have been out of position, or the cyclic regions could have been contaminated by noise.

6.2. Reconstructed bifurcation diagram.

The bifurcation parameter of the time series used in the BD reconstruction is given by

$$\rho_n = -0.2\cos(2\pi(n-1)/8) + 3.7, \ (n = 1, \cdots, 9). \tag{15}$$

To train the time-series predictors, the length of each time-series dataset was 5,000. The numbers of input, hidden, and output neurons of the time-series predictors were set to be 3, 20, and 1, respectively. The parameters σ, ζ, and ϵ of the sigmoid function were 20, 10, and 0.05, respectively.

The upper and lower panels of Fig. 6 show the reconstructed BD and the estimated Lyapunov exponents, respectively. We see that the reconstructed BD corresponds to the BD shown in Fig. 4. The bifurcation structure, such as the period-doubling bifurcations, of the reconstructed BD can be seen more clearly than it can be in the BD shown in Fig. 4. However, the reconstructed BD is more similar to the BD shown in Fig. 4 than it is to the BD shown in Fig. 5. From this result, we reason that the reconstruction of the BD identifies the target dynamical system influenced by noise.

7. Conclusion

We reconstructed a BD from time-series data generated by an electronic-circuit realization of the Rössler equations. In addition, we estimated the largest Lyapunov exponents from time-series data for the BDs. We obtained a reconstructed BD corresponding to the BD generated by the electronic circuits. The present results suggest that such BD reconstruction could be used for real-world systems. In future work, we intend to reconstruct the BDs of other electronic circuits that generate chaotic time series.

Acknowledgements

This paper was supported by a research granted from The Murata Science Foundation.

References

[1] R. Tokunaga, S. Kajiwara and S. Matsumoto, "Reconstructing bifurcation diagrams only from time-waveforms," *Physica D*, vol.79, pp.348–360, 1994.

[2] S. Ogawa, T. Ikeguchi, T. Matozaki and K. Aihara, "Nonlinear Modeling by Radial Basis Function Networks, *IEICE Trans. Fundamentals*, vol. E79-A, no.10, 1996.

[3] E. Bagarinao, K. Pakdaman, T. Nomura and S. Sato, "Reconstructing bifurcation diagrams from noisy time series using nonlinear autoregressive models," *Physical Review E*, vol.60, number 1, 1999.

[4] E. Bagarinao, K. Pakdaman, T. Nomura and S. Sato, "Time series-based bifurcation diagram reconstruction," *Physica D*, vol.130, pp.211–231, 1999.

[5] E. Bagarinao, K. Pakdaman, T. Nomura and S. Sato, "Reconstructing Bifurcation Diagrams of Dynamical Systems Using Measured Time Series," *Method Inform Med*, vol.39, pp.146–149, 2000.

[6] G. Langer and U. Parlitz, "Modeling parameter dependence from time series," *Physical Review E*, vol.70, 2004.

[7] Y. Tada and M. Adachi, "Reconstruction of Bifurcation Diagrams Using Extreme Learning Machines," *2013 IEEE International Conference on Systems, Man, and Cybernetics*, vol.79, pp.1127–1131, 2013.

[8] O. E. Rössler , "Continuous Chaos," *Ann. N. Y. Acad. Sci.31*, vol.35, pp.376-392, 1979.

[9] Y. Itoh, Y. Tada and M. Adachi, "Reconstructing bifurcation diagrams with Lyapunov exponents from only time-series data using an extreme learning machine," *Nonlinear Theory and Its Applications, IEICE*, vol.8, no. 1, pp. 2–14, 2017.

[10] A. Wolf, J. B. Swift, H. L. Swinney and J. A. Vastano, "DETERMINING LYAPUNOV EXPONENTS FROM A TIME SERIES," *Physica*, vol.16D, pp. 285–317, 1985.

[11] R. W. Preisendorfer and C. Mobley, eds, "Principal component analysis in meteorology and oceanography," Elsevier, 1988.

[12] G. B. Huang, Q. Y. Zhu and C. K. Siew, "Extreme Learning Machine: Theory and Applications," *Neurocomputing*, vol.70, pp.489–501, 2006.

[13] A Rössler Attractor Circuit, http://www.glensstuff.com/rosslerattractor/rossler.htm

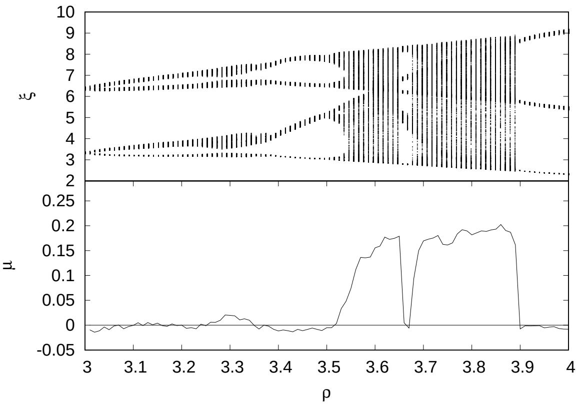

Figure 4: Bifurcation diagram generated by electronic circuits with estimated largest Lyapunov exponents.

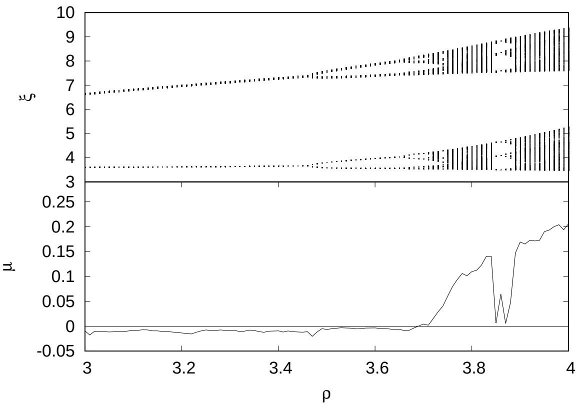

Figure 5: Bifurcation diagram generated by numerical experiments with estimated largest Lyapunov exponents.

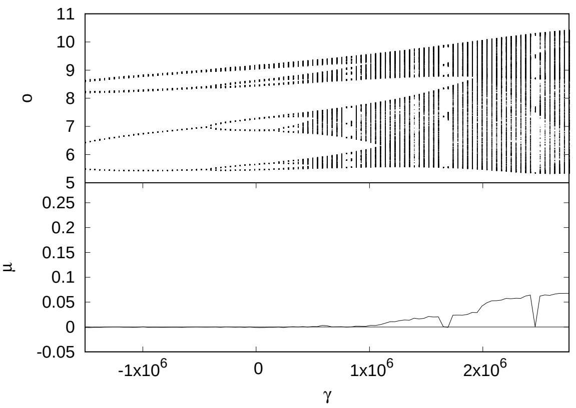

Figure 6: Reconstructed bifurcation diagram from time series data of electronic circuits with estimated largest Lyapunov exponents.